Online-Journals.org

iJIM International Journal of Interactive Mobile Technologies

iJIM | eISSN: 1865-7923 | Vol. 19 No. 9 (2025) | OPEN ACCESS

https://doi.org/10.3991/ijim.v19i09.55581

PAPER

Optimizing LiDAR Point Clouds for Mobile Digital Twin Restoration of Cultural Heritage with Trustworthy Validation

Jun Chen(✉)

College of Art and Design, Hunan First Normal University, Changsha, China

chengjun1970@hnfnu.edu.cn

ABSTRACT

The preservation and restoration of cultural heritage have long been significant endeavors throughout human history. With the rapid advancement of LiDAR technology, digital methods have become essential tools for heritage restoration. However, efficiently and accurately processing LiDAR point cloud data—particularly in mobile digital twin restoration—poses numerous challenges. Cross-scale point cloud registration and trustworthiness assessment are among the key technical hurdles. Current research methods often face trade-offs between accuracy and efficiency when handling large-scale point cloud data. Moreover, traditional centralized approaches to trustworthiness evaluation raise concerns regarding privacy protection and security. To address these challenges, this study presents two primary contributions. First, an improved PointNet-based method for cross-scale registration of LiDAR point clouds is proposed, enhancing computational efficiency while maintaining registration accuracy. Second, a novel trustworthiness scoring mechanism is introduced, leveraging federated learning to enhance the reliability of restoration results while safeguarding data privacy. These advancements not only drive forward digital twin restoration technology but also offer safer and more reliable solutions for cultural heritage preservation.

KEYWORDS

cultural heritage, digital twin restoration, LiDAR point cloud, cross-scale registration, trustworthiness scoring, federated learning

1 INTRODUCTION

Cultural heritage is an important part of human history, and preserving and restoring these heritages is of great significance for passing on culture and history [1, 2]. With the development of science and technology, digital technology has been increasingly applied in the field of cultural heritage preservation [3–6], especially LiDAR technology, which plays an important role in the three-dimensional scanning and

Chen, J. (2025). Optimizing LiDAR Point Clouds for Mobile Digital Twin Restoration of Cultural Heritage with Trustworthy Validation. *International Journal of Interactive Mobile Technologies (iJIM)*, 19(9), pp. 164–178. https://doi.org/10.3991/ijim.v19i09.55581

Article submitted 2025-01-06. Revision uploaded 2025-03-03. Final acceptance 2025-03-22.

reconstruction of cultural heritage. However, efficiently utilizing LiDAR point cloud data for the digital twin restoration of cultural heritage remains a challenge. In particular, for mobile digital twin restoration, key issues such as cross-scale registration and data trustworthiness need to be addressed.

The significance of related research lies in protecting and restoring cultural heritage through digital means, which not only improves the efficiency and accuracy of restoration but also provides abundant resources for future research and education. Achieving mobile digital twin restoration of cultural heritage helps to conduct high-precision restoration work without affecting the original artifacts [7, 8], while also facilitating remote collaboration [9, 10]. Point cloud data processing and registration based on LiDAR technology are among the core technologies to achieve this goal.

Existing research methods have made some achievements in the digital twin restoration of cultural heritage, but there are still some shortcomings and deficiencies [11–15]. For example, traditional point cloud registration methods often encounter issues of insufficient accuracy and large computational costs when handling cross-scale data [16, 17]. In addition, existing trustworthiness scoring methods typically rely on centralized data processing approaches, raising concerns about data privacy and security [18]. Koivumäki et al. [19] mentioned that traditional methods struggle to balance computational efficiency and accuracy when processing large-scale point cloud data. As for trustworthiness scoring, while Niangoran et al. [20] point out that ensuring reliability and privacy protection in centralized methods has always been a research challenge.

This paper mainly focuses on two aspects. First, an improved PointNet-based cross-scale registration method for LiDAR point clouds in mobile digital twin restoration of cultural heritage is proposed. By optimizing the PointNet model, the accuracy and efficiency of point cloud registration across different scales are improved. Second, a trustworthiness scoring mechanism for mobile digital twin restoration of cultural heritage is proposed based on federated learning, aiming to address data privacy and security issues while enhancing the trustworthiness of the scoring. Through these two aspects of research, this paper not only achieves high-precision digital twin restoration of cultural heritage in terms of technology but also provides new solutions for data security and trustworthiness, with significant academic and practical value.

2 CROSS-SCALE REGISTRATION OF LiDAR POINT CLOUDS BASED ON IMPROVED POINTNET

The core framework of the proposed cross-scale registration algorithm for LiDAR point clouds in mobile digital twin restoration of cultural heritage is based on the PointNet model, which encodes the input cultural heritage point cloud data. First, the template LiDAR point cloud and the target LiDAR point cloud of the cultural heritage are subjected to feature extraction to obtain the global feature vectors of the two-point clouds. These global feature vectors are used to preliminarily estimate the initial transformation matrix between the two-point clouds. This initial transformation matrix provides a reasonable initial estimate for the subsequent registration process, thereby narrowing the error range between the point clouds to be registered. After obtaining the initial transformation matrix, the transformed target LiDAR point cloud and the template LiDAR point clouds are input into the iterative closest point (ICP) module to further refine the initial transformation matrix. The ICP module continuously optimizes the matching relationship between point

clouds, gradually approaching the optimal registration result. During the iteration process, through multiple optimizations and updates of the transformation matrix, the algorithm accurately estimates the relative pose between the target LiDAR point cloud and the template LiDAR point cloud. The iteration continues until a preset convergence threshold is reached, indicating the completion of the registration process. Finally, the singular value decomposition (SVD) technique is used to further calculate the accurate spatial pose parameters of the cultural heritage, achieving high-precision pose estimation of unordered cultural heritage point clouds.

The algorithm incorporates a registration module whose core working principle relies on the structured light sensor model (*SAM*), which includes a feature extraction layer and a regression layer. The feature extraction layer is responsible for extracting representative geometric features from the target LiDAR point cloud O_S and the template LiDAR point cloud O_T. First, the target LiDAR point cloud and the template LiDAR point cloud are input into the PointNet module, where PointNet performs feature extraction on each point through one-dimensional convolution operations, capturing both local and global information of the point clouds. The first step of feature extraction is achieved through the T-Net module, which performs affine transformation to mitigate the effects of rotation and translation, thus providing higher rotation and translation invariance for the point cloud data. This affine transformation applies a shared multi-layer perceptron (MLP) to extract point-wise features for each point and further maps the features into a high-dimensional space. In this process, the geometric information of the point clouds is effectively captured and processed, ensuring the accuracy and stability of the features. Figure 1 illustrates the network structure of the single registration module for LiDAR point clouds.

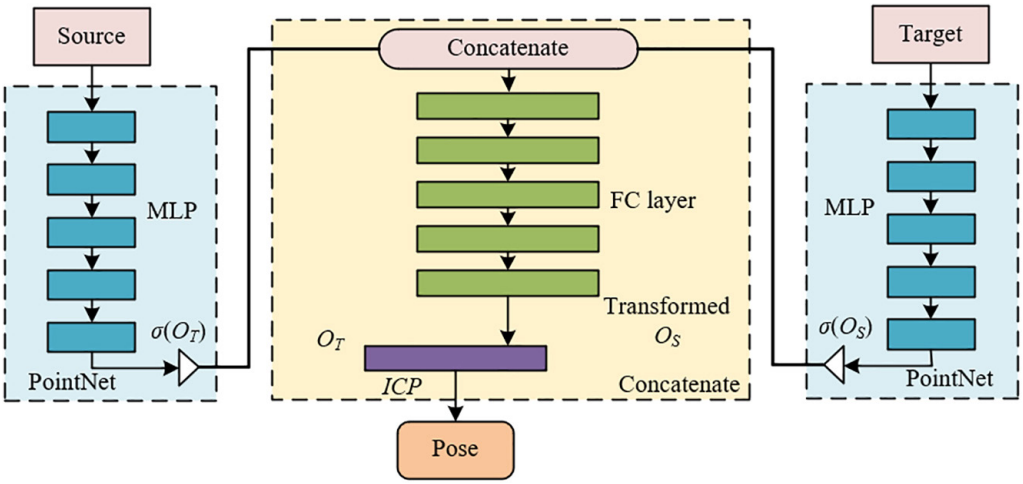

Fig. 1. Network structure of a single registration module for LiDAR point clouds

Furthermore, the output of feature extraction is aggregated into global features through max pooling operations, further extracting the global information of the LiDAR point clouds for mobile digital twin restoration of cultural heritage. To achieve precise point cloud registration, the algorithm employs a symmetric maximum set function to calculate and find the global feature vectors between the target LiDAR point cloud $\sigma(O_S)$ and the template LiDAR point cloud $\sigma(O_T)$. On this basis, the feature vectors of the target LiDAR point cloud and the template LiDAR point cloud are merged through concatenation operations to form a complete feature vector as the input of the registration module. The regression layer then predicts the transformation relationship between the target LiDAR point cloud and the

template LiDAR point cloud based on the merged feature vectors, namely the rigid transformation matrix. To improve the registration effect and avoid overfitting, the network sets five fully connected layers in the regression layer for pose estimation. Through this process, the algorithm can accurately calculate the transformation matrix between the two-point clouds, aligning the target LiDAR point cloud with the template LiDAR point cloud. Finally, the transformed target LiDAR point cloud and template LiDAR point cloud are input into the ICP module, which outputs precise 7-dimensional pose parameters, with the first three dimensions representing the position parameters and the last four dimensions representing the rotation quaternion. Figure 2 illustrates the iterative registration framework for LiDAR point clouds.

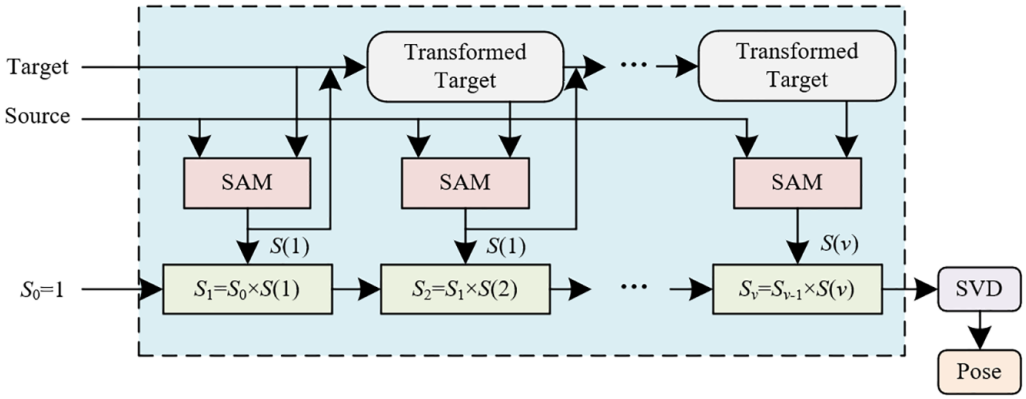

Fig. 2. Iterative registration framework for LiDAR point clouds

In the algorithm, the construction principle of the iterative registration framework fully considers the particularities of cultural heritage point cloud data, such as data sparsity, noise, outliers, occlusion, and incompleteness. To achieve precise registration of LiDAR point clouds in mobile digital twin restoration of cultural heritage under these challenging conditions, the algorithm adopts an iterative optimization approach to gradually improve registration accuracy. During each iteration, the SAM is first used to perform initial registration between the target LiDAR point cloud O_S and the template LiDAR point cloud O_T, obtaining an initial transformation matrix $S(u)$. This transformation matrix $T(i)$ represents the initial pose relationship between the target LiDAR point cloud and the template LiDAR point cloud. Then, after applying $S(u)$ to the target LiDAR point cloud, the transformed point cloud is obtained and used as input for the next SAM registration. In this way, with each iteration, the target LiDAR point cloud is gradually aligned with the template LiDAR point cloud, and the transformation matrix is continuously optimized. Through multiple iterations, the registration results of the point clouds gradually approach the precise solution until the set convergence threshold is reached, indicating that the registration process is complete. At the end of each iteration, the obtained transformation matrix $S(u)$ is used to cumulatively calculate the overall transformation matrix. The transformation matrix in each iteration updates the transformation relationship throughout the registration process through matrix multiplication. Finally, through this iterative optimization strategy, the algorithm can obtain the precise overall transformation matrix between the target LiDAR point cloud and the template LiDAR point cloud. The overall transformation between the target LiDAR point cloud and the template LiDAR point cloud is given by the following formula:

$$S = S(v) \times S(v-1) \times \ldots \times S(1) \tag{1}$$

The key to pose estimation lies in accurately extracting the rotation and translation parameters from the transformation matrix S to achieve high-precision alignment between the target LiDAR point cloud and the template LiDAR point cloud. Since cultural heritage point clouds may be affected by noise, occlusion, or incompleteness during the scanning process, the algorithm effectively eliminates these influences through the combination of iterative optimization and matrix SVD decomposition, ensuring accurate pose estimation. During the pose estimation process, the rotation matrix EEE represents the rotational relationship of the point clouds, while the displacement vector sss represents the translational displacement of the target LiDAR point cloud relative to the template LiDAR point cloud. Finally, after SVD processing, the obtained rotation matrix and displacement vector form the complete pose parameters. Let $A' = (a_u - i_a) = (a'_u)$, $O' = (a_u - i_a) = (a'_u)$, $i_a = 1/v \sum_{u=1}^{v} \|a_u\|^2$, $i_o = 1/l \sum_{u=1}^{l} \|o_u\|^2$, σ_1, σ_2, and σ_3 are eigenvalues. The complete pose parameter solution formulas are as follows:

$$\mu = \frac{1}{v} \sum_{u=1}^{v} a'_u o'^T_u = I \begin{bmatrix} \sigma_1 & 1 & 1 \\ 1 & \sigma_2 & 1 \\ 1 & 1 & \sigma_3 \end{bmatrix} N^T \tag{2}$$

$$E = NI^T, s = i_a - E_{i_o} \tag{3}$$

To effectively measure the differences between point clouds, the algorithm employs EMD as the loss function. EMD is an effective method for measuring the distance between two-point sets, particularly suitable for handling point cloud data with different shapes and structures. In the calculation of EMD, it is assumed that the target LiDAR point cloud and the template LiDAR point cloud have the same size, i.e., $|T_1| = |T_2|$, where T_1 and T_2 represent the point sets of the target LiDAR point cloud and the template LiDAR point cloud, respectively. Suppose the target LiDAR point cloud is represented by O_S^{ES}, and the template LiDAR point cloud is represented by O_T, and ϕ is the bijection relation. The EMD between the two-point clouds A and B is represented as:

$$RLF\left(O_S^{ES}, O_T\right) = \underset{\phi: O_S^{ES} \to O_T}{MIN} \frac{1}{\left|O_S^{ES}\right|} \sum_{a \in O_S^{ES}} \left\| a - \phi(a) \right\|_2 \tag{4}$$

$$M = \sum_{u=1}^{v} \eta^{V-u+1} RLF_u \left(O_S^{ES}, O_T\right) \tag{5}$$

The EMD function measures the distance between them by calculating the minimum amount of work required to "transport" each point of the target LiDAR point cloud to the template LiDAR point cloud. This measurement method effectively captures the differences in point clouds during geometric transformation. Especially in the presence of noise, outliers, or occlusion, EMD exhibits strong robustness.

3 FEDERATED LEARNING-BASED CREDIBILITY SCORING FOR MOBILE DIGITAL TWIN RESTORATION OF CULTURAL HERITAGE

To evaluate the contribution and reliability of different mobile clients in the digital twin restoration task of cultural heritage, this paper proposes a federated

learning-based credibility scoring method for mobile digital twin restoration of cultural heritage. Firstly, based on the size of the training dataset of mobile clients and the communication distance between the client and the server, the candidate mobile clients for cultural heritage digital twin restoration to participate in model aggregation are comprehensively evaluated. This evaluation process considers data volume, data quality, and communication efficiency, ensuring that the selected clients can effectively participate in the training process while minimizing delays and bandwidth bottlenecks caused by long-distance communication. By making such a selection, the efficiency of model aggregation can be improved, and the data used in the restoration process can be ensured to have high representativeness and reliability, thereby providing more accurate data support for subsequent model updates and restoration results.

Furthermore, a clustering algorithm is used to classify the candidate clients into two categories based on their similarity: benign credibility mobile clients and anomalous credibility mobile clients. Benign credibility clients usually have more complete data, good communication conditions, and significant contributions to training. In contrast, anomalous credibility clients may exhibit lower reliability due to poor data quality, high communication delays, or other factors. In this classification process, the clustering algorithm automatically identifies which clients are high-quality data providers by analyzing the similarity of features between clients. Finally, the credibility score is determined based on the ratio of benign credibility clients to anomalous credibility clients. This method enables the dynamic evaluation of each client's contribution during training, ensuring that high-quality data providers and stable training results are prioritized in model aggregation. Consequently, the accuracy and robustness of cultural heritage digital twin restoration can be further improved. The design of this scoring mechanism contributes to enhancing the efficiency and precision of model updates in federated learning, particularly when dealing with a large number of decentralized and highly heterogeneous mobile clients.

3.1 Mobile client selection

The principle of selecting mobile clients for cultural heritage digital twin restoration focuses on comprehensively evaluating client effectiveness and optimizing client selection based on data volume and communication efficiency. In the federated weighted averaging algorithm, the weight of a client is typically determined based on the amount of data it holds, meaning that clients with larger data volumes have a greater impact on the global model. However, this paper further considers communication consumption, particularly in clients with smaller data volumes, whose parameter updates may be minimal but whose communication overhead may significantly affect the overall model training.

In the actual client selection process, each mobile client for cultural heritage digital twin restoration is assigned a triplet (F, T, R), where F represents the data volume of the client, T is the communication distance, and R is the client status. This triplet comprehensively reflects the current state of the client. Before each round of data exchange begins, the server evaluates each client based on the triplet information. Then, a weighted summation method is used to calculate the evaluation value for each client, where a higher evaluation value indicates a greater contribution to the global model and higher communication efficiency. The calculation process is as follows, where a and b are weights, and φ represents the evaluation value of the client:

$$F' = \frac{F - F_{MIN}}{F_{MAX} - F_{MIN}} \tag{6}$$

$$T' = \frac{T_{MAX} - T_{MIN}}{T_{MAX} - T_{MIN}} \tag{7}$$

$$(F, T, R) \rightarrow \varphi = (a \times F' + b \times T') \times R \tag{8}$$

The server sorts the evaluation values of all cultural heritage mobile digital twin restoration mobile clients $\{\varphi_1, \varphi_2, \varphi_3..., \varphi_l\}$ from highest to lowest, selecting a fixed number of top-performing cultural heritage mobile digital twin restoration mobile clients to participate in this round of communication.

3.2 Similarity-based mobile client clustering

Further filtering these cultural heritage mobile digital twin restoration mobile clients, this paper identifies and filters out potential malicious clients by evaluating the difference between each cultural heritage mobile digital twin restoration mobile client and the global model during the training process. In each iteration round, the server calculates Q'_u, which represents the difference between the local model parameters $Q_{LO,u}$ of each client and the global model parameters $Q_{GL,u}$. This difference reflects the degree of change between the client's local model and the global model. Since normal cultural heritage mobile digital twin restoration mobile client models exhibit similar convergence trends, their Q'_u values should be close. However, malicious clients often deliberately tamper with local model parameters, resulting in a larger Q'_u value compared to other normal clients. The server performs Z-score normalization on these difference values to ensure that original model information is not leaked during data transmission, making subsequent similarity calculations more convenient. The Z-score normalized values reflect the similarity between the client's local model and the global model, providing a reliable basis for the clustering algorithm.

$$T = NORM(Q'_u) = NORM(Q_{GL,u} - Q_{LO,u}) \tag{9}$$

Furthermore, cosine similarity is used to calculate the similarity between different cultural heritage mobile digital twin restoration mobile clients:

$$SIM = \frac{x * y}{\|x\| \times \|y\|} = \frac{\sum_{u=1}^{v} (a_u \times b_u)}{\sqrt{\sum_{u=1}^{v} (a_u)^2} \times \sqrt{\sum_{u=1}^{v} (b_u)^2}} \tag{10}$$

$$SIM_{i,n} = \frac{S_i^{1-DIMENSION} * S_n^{1-DIMENSION}}{\left\|S_i^{1-DIMENSION}\right\| \times \left\|S_n^{1-DIMENSION}\right\|} \tag{11}$$

Based on the similarity of each client, the server uses the K-means clustering algorithm to group all cultural heritage mobile digital twin restoration mobile clients. K-means clustering assigns clients with high similarity to the same group, while clients with low similarity are assigned to different groups. Under normal circumstances, most cultural heritage mobile digital twin restoration mobile clients should

be classified as the "benign" group. These clients exhibit smaller Q'_u differences over multiple iterations, with models gradually stabilizing. In contrast, the abnormal group includes two scenarios: one is temporary model differences due to data heterogeneity or the first-time participation in the federated learning process, where these clients' model differences gradually decrease with iterations and eventually get classified into the benign group; the other is malicious clients, who intentionally tamper with model parameters, showing large Q'_u differences over multiple iterations, which do not decrease over time and may even increase. The server tracks the behavior of clients in the abnormal group. When a client's abnormal record exceeds a set threshold, the server marks it as a malicious client, prohibiting its participation in subsequent federated learning processes.

3.3 Negotiated mask

To ensure data privacy and security during the federated learning process, this paper introduces the negotiated mask, aiming to protect the local data of cultural heritage mobile digital twin restoration mobile clients through encryption technology. In each round of model training, clients negotiate with other clients to generate unique mask parameters. This process is based on session key exchange between clients, ensuring that each pair of clients has a private key. By using this key as a random seed, clients generate random numbers and apply these numbers to mask their model parameters, transforming them into obfuscated parameters. These obfuscated parameters are uploaded to the server, preventing the server from directly accessing the original gradients or model parameters. Instead, the server can only aggregate the masked data.

The negotiated mask not only enhances the security of model training but also effectively protects the privacy of participating clients in the cultural heritage mobile digital twin restoration process. The mask negotiated by each client ensures that the uploaded gradients or model parameters are obfuscated, yet due to the additive aggregation property, the aggregated result at the server is identical to the result calculated with the original data. Specifically, each pair of clients conducts a mask negotiation $T_{i,n}$, and after completing the negotiation with other clients, the parameters transmitted by each cultural heritage mobile digital twin restoration mobile client become:

$$B_i = A_i + \sum_{n\in I, i<n} T_{i,n} - \sum_{n\in I, i>n} T_{i,n} \tag{12}$$

All cultural heritage mobile digital twin restoration mobile clients upload the obfuscated parameters. Upon receiving them, the server performs additive parameter aggregation to obtain:

$$c = \sum_{i\in I} B_i = \sum_{i\in I, i<n} \left(A_i + \sum_{n\in I, i<n} T_{i,n} - \sum_{n\in I, i>n} T_{i,n} \right) = \sum_{i\in I} A_i \tag{13}$$

In this way, the server can only observe the aggregation result and cannot infer individual client data. This mechanism prevents malicious clients from attacking the global model by tampering with data, thereby enhancing the robustness of federated learning and ensuring the security of data and the reliability of credibility scoring in the cultural heritage digital twin restoration process.

3.4 Secure aggregation protocol

To ensure the privacy and security of cultural heritage mobile digital twin restoration mobile clients during model parameter aggregation, this paper introduces a secure aggregation protocol based on secure multi-party computation. To achieve this goal, this paper first classifies and filters the cultural heritage mobile digital twin restoration mobile clients into benign clients and abnormal clients. Benign clients are those that exhibit consistency and stability during the training process, while abnormal clients may include malicious clients or clients with abnormal behavior due to data heterogeneity. The server sums the parameters $Q_{s,u}$ from both benign and abnormal client classes and divides by the number of participating clients j, yielding the model parameter q_{s+1} as the global model for the next round:

$$q_{s+1} = \frac{\sum_{u=1}^{j} q_{s,u}}{j} \tag{14}$$

During the aggregation process of benign clients, the negotiated mask exchange technology is adopted for secure aggregation. Specifically, each benign client establishes a ring connection with other clients in the same group and exchanges masks with its preceding and succeeding neighbor nodes. In this way, the local model parameters of each client are masked, forming obfuscated parameters. Although the server receives obfuscated parameters, due to the nature of additive parameter aggregation, the final aggregation result is consistent with the result calculated using the original parameters. The server cannot infer the true data of any single client by observing its parameters, thereby effectively protecting the privacy of the clients. Additionally, because the clients within the same group have smaller differences in model parameters, the mask exchange among them makes the obfuscated parameters more difficult to distinguish, further enhancing the security of privacy protection.

For abnormal clients, due to the possibility of malicious behavior, the study applies parameter substitution on top of secure aggregation to reduce their contribution to the global model update. Specifically, before uploading, the parameters of abnormal clients are replaced with standard parameter values to prevent the impact of data poisoning attacks on the global model. This method ensures that, although abnormal clients participate in the federated learning process, their negative impact on the global model is minimized. Finally, the server performs additive parameter averaging separately on the parameters from benign and abnormal clients to form the global model for the next round. Through this secure aggregation protocol, the study not only guarantees the privacy and data security of cultural heritage mobile digital twin restoration mobile clients but also improves the reliability and robustness of the global model, effectively achieving the goal of credibility scoring.

4 EXPERIMENTAL RESULTS AND ANALYSIS

From the experimental results table shown in Figure 3, it can be observed that the performance of various point cloud registration methods differs significantly under different noise levels. As the standard deviation of Gaussian noise increases, the performance of all methods declines, but the extent of the decline varies among different methods. The ICP method shows the most instability, with its ICP value

dropping to 0.14 when the noise level is 0.2, compared to an ICP value of 0.6 when there is no noise. This indicates that the ICP method is highly susceptible to high-noise environments. In contrast, the normal distributions transform (NDT) method exhibits relatively strong robustness, with its performance declining slightly as the noise level increases from 0 to 0.2, reaching a minimum of 0.11. The generalized ICP (GICP) method shows similar behavior to NDT but with a slightly smoother downward trend. The global optimal ICP (Go-ICP) method maintains relatively high performance even under higher noise levels, though it performs slightly worse than NDT and GICP. The method proposed in this paper delivers the best registration result when the noise level is 0 (value of 1), but its performance gradually declines as noise increases. Particularly when the noise standard deviation reaches 0.2, its value drops to 0.06, demonstrating strong robustness against noise.

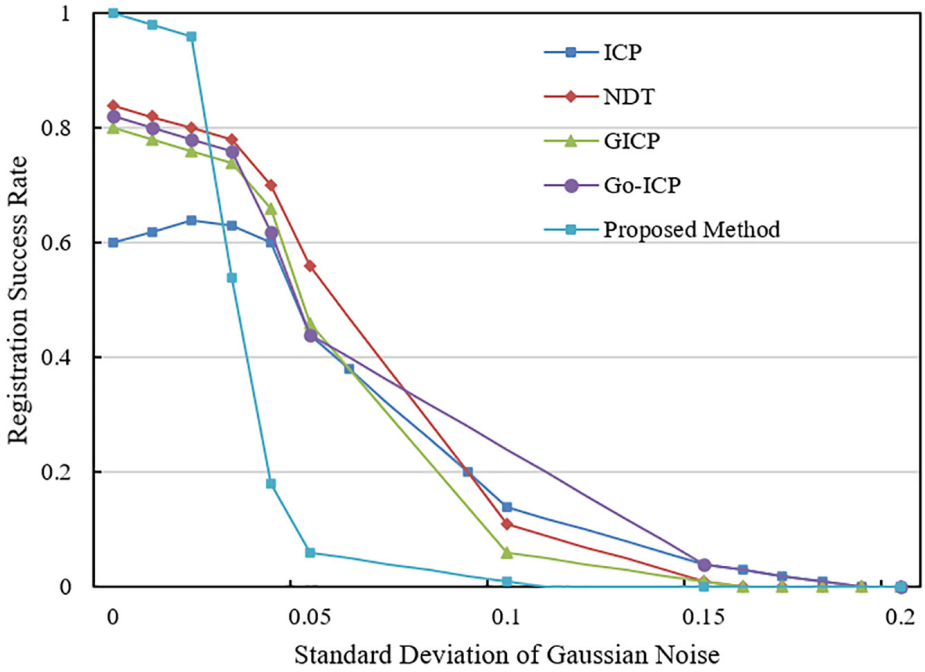

Fig. 3. Performance of various LiDAR point cloud registration methods under different levels of Gaussian noise

Table 1. Registration test results for different levels of incomplete LiDAR point clouds

Completeness	*Errr* (*E*)	*Errr* (*s*)	E (MSE, MAE)	s (MSE, MAE)
94%	3.526	0.185	(4.125,2.215)	(0.215,0.125)
91%	5.214	0.284	(6.125,3.562)	(0.216,0.147)
76%	7.785	0.312	(9.125,5.231)	(0.328,0.221)
61%	9.230	0.412	(11.245,7.125)	(0.348,0.241)
51%	11.235	0.658	(12.578,8.236)	(0.418,0.378)
24%	18.265	0.754	(22.315,13.265)	(0.615,0.387)

From the data shown in Table 1, it can be observed that as the LiDAR point cloud incompleteness increases, the registration accuracy gradually decreases. Specifically, when the completeness is 94%, the rotation error *Errr*(*E*) is 3.526, and the translation error *Errr*(*s*) is 0.185. The MSE and MAE are (4.125, 2.215) and (0.215, 0.125),

respectively, demonstrating highly accurate registration results. As completeness decreases to 91%, 76%, 61%, 51%, and 24%, the rotation error and translation error gradually increase, and MSE and MAE also show corresponding upward trends. Particularly when the completeness is 24%, the rotation error rises to 18.265, the translation error reaches 0.754, and the MSE and MAE increase to (22.315, 13.265) and (0.615, 0.387), respectively. This indicates that registration accuracy significantly declines under high levels of incompleteness. These results reflect that the degree of point cloud incompleteness has a significant impact on registration performance. As the number of missing point increases, the rise in rotation and translation errors is inevitable. The following conclusions can be drawn: at higher levels of point cloud completeness, the proposed method effectively reduces rotation and translation errors, achieving the best registration accuracy when completeness is 94%. As point cloud incompleteness increases, although the errors rise, the proposed method maintains relatively stable performance. Compared to traditional methods, the rotation and translation errors remain relatively small when handling LiDAR point clouds with varying levels of completeness. Particularly for low-completeness point cloud data, the proposed method effectively reduces rotation and translation errors through cross-scale registration optimization, indicating that the improved PointNet model has strong robustness and can effectively enhance point cloud registration accuracy in cultural heritage digital twin restoration.

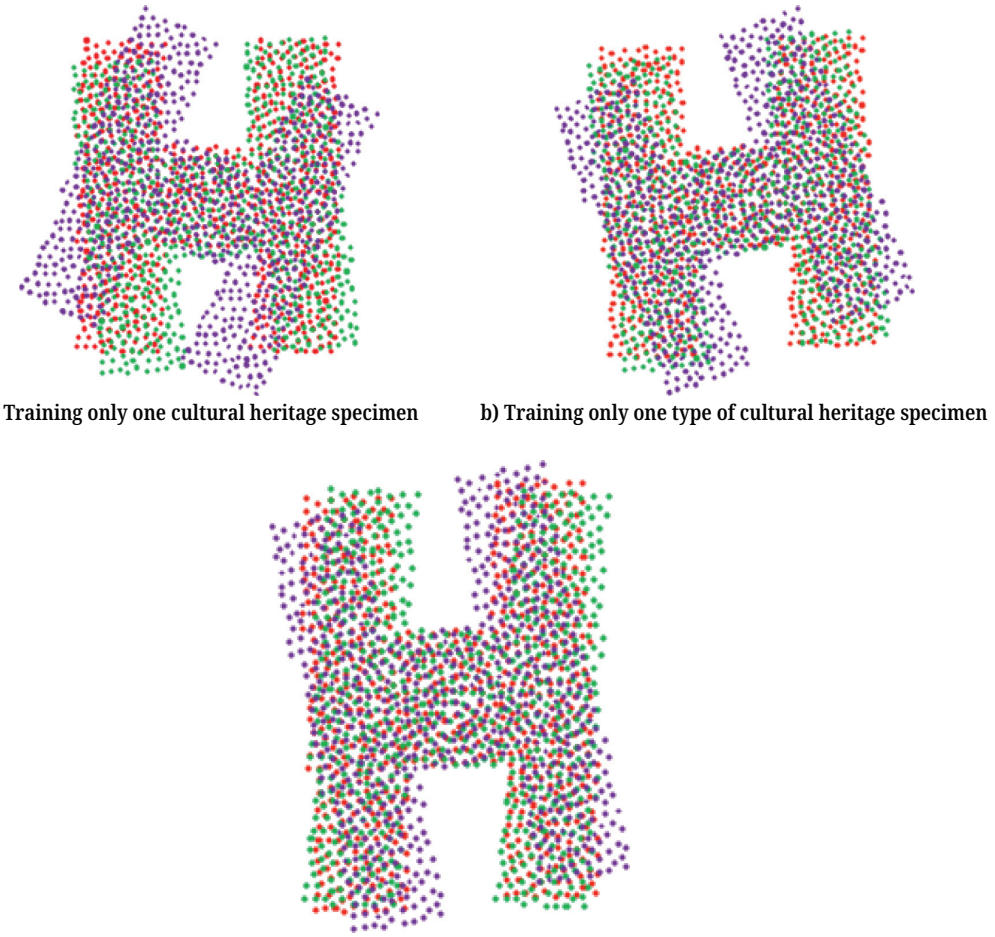

a) Training only one cultural heritage specimen

b) Training only one type of cultural heritage specimen

c) Training multiple types of cultural heritage specimens

Fig. 4. Point cloud registration results of cultural heritage specimens under different categories with the ICP module

Fig. 5. Point cloud registration results of cultural heritage specimens with Gaussian noise using the proposed method

Figures 4 and 5, respectively, show the results of point cloud registration of cultural heritage specimens using the ICP module and the proposed method under different categories. In the experiment, the ICP module performed eight iterations and finally completed the point cloud registration successfully. However, its rotation and displacement errors were relatively large, and the registration efficiency was low. This is because the ICP method requires multiple iterations to achieve better accuracy, making the process slow in complex scenarios, especially when handling point clouds with significant missing data, rendering the registration process inefficient. In contrast, the proposed point cloud optimization method showed superior performance when handling minor missing data. The successfully registered point cloud results demonstrated that the rotation and displacement errors were significantly smaller. Additionally, the experiment revealed that when large occlusions were present in the point cloud, the errors increased due to the loss of contour features, indicating that the proposed method still faces challenges in such scenarios.

Table 2. Accuracy comparison of credibility scoring under different federated learning schemes

Method	Stv	Test Accuracy		
		avgn = 2	avgn = 3	avgn = 4
Local	1	82.321(± 0.01)	80.215(± 0.012)	82.241(± 0.061)
	2	82.369(± 0.01)	82.315(± 0.012)	82.487(± 0.012)
FedAvg	1	91.254(± 1.155)	92.325(± 1.241)	91.201(± 0.856)
	2	91.245(± 0.885)	92.332(± 2.210)	91.235(± 1.125)
FedProto	1	91.585(± 0.321)	93.214(± 0.235)	91.258(± 0.623)
	2	92.321(± 0.098)	92.321(± 0.114)	93.265(± 0.441)
Proposed Method	1	92.325(± 0.072)	94.252(± 0.256)	88.245(± 0.326)
	2	92.336(± 0.087)	94.589(± 0.092)	92.365(± 0.179)

From the data in Table 2, it can be observed that different federated learning schemes exhibit noticeable differences in the accuracy of credibility scoring for cultural heritage digital twin restoration. Specifically, the local method shows relatively

low-test accuracy, especially in the cases of avgn = 2 and avgn = 4, where the accuracy is 80.215 and 82.241, respectively, with slight fluctuations. Under the FedAvg scheme, although its accuracy is relatively high, particularly when avgn = 3, reaching 92.325, its fluctuation is large, and the standard deviation is higher, indicating a certain degree of instability. In contrast, the FedProto method shows relatively stable and high accuracy in all cases, especially when avgn = 2, where the accuracy reaches 92.321 with a smaller standard deviation, highlighting its advantage in federated learning schemes. Finally, the proposed method exhibits excellent test accuracy in all cases, particularly when avgn = 2, where the accuracy reaches 94.589, with a smaller standard deviation, demonstrating higher stability and reliability.

5 CONCLUSION

This paper proposed two core technologies: a cross-scale registration method based on improved PointNet and a credibility scoring mechanism based on federated learning. In terms of point cloud registration, the optimization of the PointNet model effectively improved the accuracy and efficiency of point cloud registration across different scales, especially in handling LiDAR point cloud data for cultural heritage restoration. It better addressed issues such as data loss and occlusion. The introduction of the federated learning method resolved the data privacy and security issues faced by traditional methods, ensuring data protection during cultural heritage restoration while enhancing the credibility of the scoring mechanism. Experimental results show that the proposed improved method surpasses traditional methods in terms of accuracy, stability, and robustness, particularly in point cloud loss and high-noise environments, demonstrating strong application value.

Although this study has made certain advancements in the field of cultural heritage restoration, it still has limitations. First, although the cross-scale registration method performs well in most cases, errors increase when dealing with large-scale occlusions or severely missing point cloud data. Second, while the federated learning scheme effectively improves the accuracy of credibility scoring, it may still lead to certain biases and instabilities in cases where data distribution among devices is uneven or there are significant differences in device performance. Therefore, future research can further optimize the cross-scale registration method, explore more effective occlusion and loss handling strategies, and improve registration accuracy in extreme cases. Additionally, more robust federated learning frameworks can be developed to reduce the impact of uneven data distribution on training results and enhance model adaptability and reliability. Furthermore, as the demand for digital twin restoration of cultural heritage diversifies, integrating more intelligent technologies, such as deep learning and multimodal data fusion, to further improve restoration outcomes will become a crucial direction for future research.

6 REFERENCES

[1] H. K. Tenh and N. Shiratuddin, "Components of adaptive augmented reality model for heritage mobile application," *International Journal of Interactive Mobile Technologies (iJIM)*, vol. 16, no. 2, pp. 17–27, 2022. https://doi.org/10.3991/ijim.v16i02.27317

[2] S. Öztemiz, "Cultural heritage literacy: A survey of academics from humanities and social sciences," *Journal of Librarianship and Information Science*, vol. 52, no. 3, pp. 818–831, 2019. https://doi.org/10.1177/0961000619872529

[3] N. Aziz, S. S. Hamzah, S. Z. Ahmad, W. Matcha, and S. Binsaleh, "Augmented reality mobile application for promoting culture and heritage in Thailand and Malaysia: The prototype development and heuristic evaluation," *International Journal of Interactive Mobile Technologies (iJIM)*, vol. 18, no. 14, pp. 72–89, 2024. https://doi.org/10.3991/ijim.v18i14.48381

[4] I. Nishanbaev, E. Champion, and D. A. McMeekin, "A web GIS-based integration of 3D digital models with linked open data for cultural heritage exploration," *ISPRS International Journal of Geo-Information*, vol. 10, no. 10, p. 684, 2021. https://doi.org/10.3390/ijgi10100684

[5] S. R. A. Al-Timimy and B. A. H. Bedewy, "Enhancing urban sustainability by integrating MCDM and model of GIS spatial analysis in Al-Nasiriyah Heritage center development," *International Journal of Sustainable Development and Planning*, vol. 18, no. 11, pp. 3429–3438, 2023. https://doi.org/10.18280/ijsdp.181108

[6] G. Neglia, M. Angrisano, I. Mecca, and F. Fabbrocino, "Cultural Heritage at risk in world conflicts: Digital tools' contribution to its preservation," *Heritage*, vol. 7, no. 11, pp. 6343–6365, 2024. https://doi.org/10.3390/heritage7110297

[7] M. Hou, S. Yang, Y. Hu, Y. Wu, Z. Shu, and X. Zhang, "A novel method for the virtual restoration of cultural relics based on a 3D fine model," *Dyna*, vol. 90, no. 3, pp. 307–313, 2015. https://doi.org/10.6036/7538

[8] P. Zhao, Y. S. Zhang, Y. Shen, X. J. Li, P. P. Zhu, and W. W. Zhu, "Advancements in artificial hydraulic lime composites for sustainable restoration of stone cultural heritage," *Science of Advanced Materials*, vol. 15, no. 12, pp. 1681–1689, 2023. https://doi.org/10.1166/sam.2023.4607

[9] X. Sun, J. Jia, P. Xu, J. Ni, W. Shi, and B. Li, "Structure-guided virtual restoration for defective silk cultural relics," *Journal of Cultural Heritage*, vol. 62, pp. 78–89, 2023. https://doi.org/10.1016/j.culher.2023.05.016

[10] E. Diz-Mellado, J. Perez-Fenoy, M. Mudarra-Mata, C. Rivera-Gómez, and C. Galan-Marin, "Enhancing 3D-printed clay models for heritage restoration through 3D scanning," *Applied Sciences*, vol. 14, no. 23, p. 10898, 2024. https://doi.org/10.3390/app142310898

[11] F. Cinquepalmi and V. A. Tiburcio, "Sustainable restoration of cultural heritage in the digital era," *Vitruvio*, vol. 8, no. 2, pp. 76–87, 2023. https://doi.org/10.4995/vitruvio-ijats.2023.20545

[12] S. Bruno, A. Scioti, A. Pierucci, R. Rubino, T. Di Noia, and F. Fatiguso, "VERBUM – virtual enhanced reality for building modelling (virtual technical tour in digital twins for building conservation)," *Journal of Information Technology in Construction*, vol. 27, pp. 20–47, 2022. https://doi.org/10.36680/j.itcon.2022.002

[13] E. Doria and M. Morandotti, "Documentation, conservation, and reuse planning activities for disused cultural heritage," *VITRUVIO-International Journal of Architectural Technology and Sustainability*, vol. 8, pp. 30–47, 2023. https://doi.org/10.4995/vitruvio-ijats.2023.18814

[14] A. Makovetskii, S. Voronin, V. Kober, and A. Voronin, "Registration algorithm for incongruent point clouds," in *2022 VIII International Conference on Information Technology and Nanotechnology (ITNT)*, Samara, Russian Federation, 2022, pp. 1–8. https://doi.org/10.1109/ITNT55410.2022.9848569

[15] B. Lipuš and B. Žalik, "3D convex hull-based registration method for point cloud watermark extraction," *Sensors*, vol. 19, no. 15, p. 3268, 2019. https://doi.org/10.3390/s19153268

[16] M. J. Bark *et al.*, "Evaluation of the impact of orthodontists' smile with malocclusions on social media and professional credibility," *Clin Oral Invest*, vol. 28, p. 74, 2024. https://doi.org/10.1007/s00784-023-05416-1

[17] R. G. Negri, L. A. T. Machado, S. English, and M. Forsythe, "Combining a cloud-resolving model with satellite for cloud process model simulation validation," *Journal of Applied Meteorology and Climatology*, vol. 53, pp. 521–533, 2014. https://doi.org/10.1175/JAMC-D-12-0178.1

[18] L. Gugerty and D. M. Link, "How heuristic credibility cues affect credibility judgments and decisions," *Journal of Experimental Psychology: Applied*, vol. 26, no. 4, pp. 620–645, 2020. https://doi.org/10.1037/xap0000279

[19] P. Koivumäki, G. Steinböck, and K. Haneda, "Impacts of point cloud modeling on the accuracy of ray-based multipath propagation simulations," *IEEE Transactions on Antennas and Propagation*, vol. 69, no. 8, pp. 4737–4747, 2021. https://doi.org/10.1109/TAP.2021.3050482

[20] S. Niangoran, V. Journot, O. Marcy, X. Anglaret, and A. Alioum, "Performance of four centralized statistical monitoring methods for early detection of an atypical center in a multicenter study," *Contemporary Clinical Trials Communications*, vol. 34, p. 101168, 2023. https://doi.org/10.1016/j.conctc.2023.101168

7 AUTHOR

Jun Chen graduated from Hunan Normal University in 1996 and works at College of Art and Design, Hunan First Normal University, engaged in art education work (E-mail: chengjun1970@hnfnu.edu.cn; ORCID: https://orcid.org/0009-0008-0565-7024).